POAC'15
Trondheim, Norway

Proceedings of the 23rd International Conference on
Port and Ocean Engineering under Arctic Conditions
June 14-18, 2015
Trondheim, Norway

Experimental and numerical investigation on ice submerging for icebreaker with 2D model test using synthetic ice

Junji Sawamura[1], Shinji Kioka[2] and Akihisa Konno[3]
[1] Department of Naval Architecture and Ocean Engineering, Osaka University, JAPAN
[2] Civil Engineering Research Institute for Cold Region, JAPAN
[3] Department of Mechanical Engineering, Kogakuin University, JAPAN

ABSTRACT
2D model test using synthetic ices have been carried out in order to provide information on ice submerging regarding an icebreaker advancing into level ice. A polypropylene plate has been used for a synthetic ice. The ship was rigidly towed by the carriage and advances in pre-sawn ice with the constant speed. The ice forces and the motions of ice submerging in different ship and ice conditions such as the ship speed and size of the pre-swan ice were measured. The measured data showed the motions and the ice forces of ice submerging depend on the geometrical conditions between the ship and the pre-sawn ice as well as the ship speed. 2D numerical model that enables simulations of ice force on the icebreaker that is advancing into pre-sawn ices were developed by physically based modelling. The contact force and the friction force act on the contact point between ship and ice. Buoyancy and fluid force described by the simple formula were considered as the hydrodynamic force acting on the ice floe. The numerical results are compared with experimental data. The ice force of the ice submerging of the numerical results roughly agreed with the experimental data qualitatively. The influence of the ship and ice conditions on the ice submerging are investigated. The hydrodynamic force induced by the ice submerging are important role to estimate the ice force as well as friction force.

INTRODUCTION
In order to improve the structural components and maneuverability of the ice-going vessels, it is vital issue to estimate the ice force (pressure) distributions acting on the ship. The model tests and full-scale measurements have been generally used to evaluate the performance and estimate the ice force for the ice-going ships. A local ice force on the hull is implicitly estimated by the structural response derived by the strain gages on the structural members in the full-scale measurement (e.g. Frederking, 2003). The panel censers installed on the outer hull is used to measure the local ice pressure on the hull (e.g. Izumiyama *et al.*, 1999). The data obtained from the full-scaled measurements and the model tests were not enough to investigate the detail of the local ice force due to the limitations of special and time resolution of the measurement system and the cost inefficiency of full-scale measurements and the model tests using the ice tank. The distributions of the local ice force around a ship hull, therefore, have not been fully understood yet.

The synthetic ice is alternatively used for model tests in towing tank with instead of the refrigerated ice in the ice tank. The synthetic ice is made of artificial material such as polypropylene or paraffin wax. The size and shape of a synthetic ice can be easily controlled. A synthetic ice can be used repeatedly. Therefore, the model test using synthetic ice is cost

efficient. There is little limitation of the experimental conditions in the model test using synthetic ice. There are few studies done related to the experiments using synthetic ice. Song Y.Y., *et al*., (2007) conducted the model test in a towing tank using a wax type synthetic ice with similar density and the friction to those of refrigerated ice. The ice resistance in pack ice conditions were measured. Overall tendency of the ice resistance in pack ice conditions showed the good agreement. It was shown that the model test with synthetic ice instead of refrigerated ice in an ice tank is a useful for model test in pack ice conditions.

Ice breaking process for an icebreaker advancing into level ice can be divided into two phases. First, the ice cover is broken into relatively small cusps at waterline when the icebreaker collides with the edge of the ice cover. Second, the broken cusp is rotating and sliding along the hull as the icebreaker further advances. The total ice force finally can be calculated by the sum of breaking force and ice submerging force. Valanto (1992) have conducted two-dimensional experiments and developed the numerical model for ship advancing into a level ice. The transit response of a floating ice sheet were focused on. The dynamic bending failure and the rotation of the broken ice floes were estimated. Puntigliano (1997) carried out the model test to investigate physical phenomena of ice sliding contributing to ice resistance under the design waterline. Konno *et al*., (2006) numerically predicted ice clearing force as an icebreaker is advancing into brash ice channel. Sawamura *et al*., (2011) and Sawamura (2015) developed the numerical model that predicts the repetitive icebreaking of the plate ice and rotating and sliding of the broken cusp when an icebreaker is advancing into level ice. The numerical method of Sawamura (2015) is divided into two phase according to the icebreaking phenomena of icebreaker. The icebreaking pattern and ice force distribution of the dynamic bending failure of the floating ice cover is calculated by using the ship-ice contact detection technique and bending behaviour of the simulated by fluid-structure interaction to represent the dynamic response of fluid underneath the floating ice plate. The rotating and sliding of the broken cusp are described by rigid body equations based on physically based modelling. The ice submerging force can be treated as the contact force and friction force between ship and ice. The total ice force under the waterline can be obtained by the sum of the breaking force and submerging force.

This paper focuses on ice submerging after an icebreaker breaks a floating ice cover. The ice submerging is treated as the icebreaker advances into the pre-sawn ice. The ice force and the motions of rotating and sliding of pre-sawn ice are investigated both experimentally and numerically. 2D model tests using synthetic ice made by polypropylene plate are conducted to provide information of physical phenomena of ice submerging. The ice force and motions of the broken cusp in different ship and ice conditions were measured. Although the experiments are conducted in two dimension and synthetic ices are used instead of the refrigerated ice, the model tests gives us clear understanding of the physical behaviour of the broken cusp induced by the interactions between ship and broken cusp. 2D numerical model that enables simulations of the ice force on the icebreaker advancing into pre-sawn ices was developed to represent the ice force obtained in the 2D model experiments. The numerical results are compared with experimental data. The ice force of ice submerging in the numerical results roughly agreed with the experimental data. The numerical model, together with experiments, is capable of clarifying dominant component in ice submerging contributing to the ice force.

2D MODEL TEST

The experiments were conducted at the 2D water tank in Civil Engineering Research Institute for Cold Region, JAPAN. The tank is 20.00m in length, 0.75m in width and 0.90m in depth.

The tank was divided by the partition board. The dimension of the tank used for the 2D model experiments is 10.00m in length, 0.40m in width and 0.90m in depth. 2D simplified icebreaker model was designed and was made of polyvinyl chloride boards. The principal dimension of the model is 1.00m in length, 0.33m in width and 0.057m in draft. The width of the model was enough wide to keep small the effects of leakage in the small gaps between the sidewall of the tank, but narrow enough to ensure the 2D motions of the ice floes and flow of surrounding water. The length of the flat bottom of the model is 0.40m. The model was designed that the both side can be used for the bow. The angle of the between the bow plate and the water line were 15° and 25°. A polypropylene board (NAC RH - PP, NAC KS. Co., Ltd) was used for the synthetic ice. The density of polypropylene board is 910 kg/m^3. The friction coefficient between the model (polyvinyl chloride) and the ice (polypropylene) were not measured, but 0.45 (PVC) and 0.3 (PP) in their catalog, respectively. The flexural strength of the synthetic ice has not been considered in the experiments, since the experiments were conducted in pre-sawn ice. Figure 1 shows a schematic of the experimental setup. The model was rigidly attached to the towing carriage via towing rod. Total resistance of the model in surge (x) and heave (z) direction were measured by the force transducer attached to the towing rod. The distance of the model advancing was measured by the displacement gauge. The resistance and displacement were measured with sampling rate of 100Hz.The ice submerging were observed through the transparent sidewall. The motion of ice cups were recorded by the four cameras (bow, midship, aft and whole ship). The tactile censer (I-Scan201, NITTA Corporation) was attached to the bow plate to measure the distributions of the local ice pressure. In this paper the ice pressure measured by the tactile censer have not been shown due to the limitation of the number of pages. The synthetic ices were formed into rectangular plate. The ices were arranged on the water surface in 100% concentration. The tests were performed for ice thickness of 0.005m, 0.010m and 0.020m, and for ice length of 0.050m, 0.010m and 0.020m. The model was towed with the constant speeds of 0.040m/s, 0.158m/s and 0.392m/s. Table 1 summarizes the test conditions. The experiment repeats 3 times for each test conditions to verify the repeatability of the measurement.

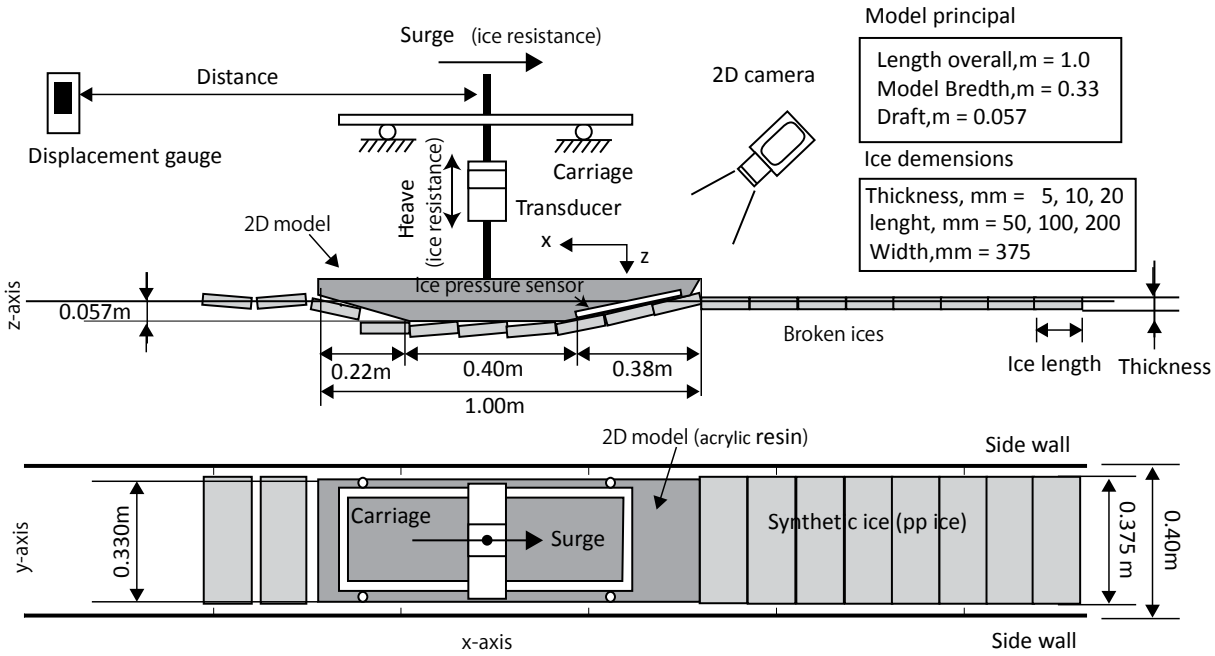

Figure 1 Experimental Set-up.

Table 1. Summary of test conditions.

Test No.	Ship conditions		Ice conditions	
	Velocity (m/s)	Bow angle (deg.)	Thickness (m)	Length (m)
Case 01	0.040 (Low)	15		
Case 02	0.158 (Middle)	15		
Case 03	0.392 (High)	15		
Case 04	0.040 (Low)	15	0.010	0.100
Case 05	0.158 (Middle)	15	0.010	0.100
Case 06	0.392 (High)	15	0.010	0.100
Case 07	0.040 (Low)	15	0.020	0.100
Case 08	0.158 (Middle)	15	0.020	0.100
Case 09	0.392 (High)	15	0.020	0.100
Case 10	0.040 (Low)	15	0.005	0.100
Case 11	0.158 (Middle)	15	0.005	0.100
Case 12	0.392 (High)	15	0.005	0.100
Case 13	0.040 (Low)	15	0.010	0.200
Case 14	0.158 (Middle)	15	0.010	0.200
Case 15	0.392 (High)	15	0.010	0.200
Case 16	0.040 (Low)	15	0.010	0.050
Case 17	0.158 (Middle)	15	0.010	0.050
Case 18	0.392 (High)	15	0.010	0.050
Case 19	0.040 (Low)	25	0.010	0.100
Case 20	0.158 (Middle)	25	0.010	0.100
Case 21	0.392 (High)	25	0.010	0.100

The total ice resistance force in level ice can be expressed by the following equations (Enkvist, E., 1972):

$$R_T = R_B + R_S + R_V + R_W , \quad (1)$$

where, R_T = Total Icebreaking Resistance,

R_B = Pure Icebreaking Resistance,

R_S = Submerging Resistance,

R_V = Velocity Dependent Resistance,

R_W = Water Resistance.

The pre-sawn ice test are conducted to measure the sum of the submerging, velocity dependent and water resistance ($R_S + R_V + R_W$), except pure icebreaking resistance. The water resistance (R_W) can be obtained by the open water test. Thus, the sum of the submerging and velocity dependent resistance ($R_S + R_V$) can be obtained by subtracting the measured resistance of the open water test from one of the pre-sawn ice test in the same ship conditions. In this paper, the open water tests (Case01, 02 and 03) were carried out. The submerging and velocity dependent force were obtained by subtracting the ice force measured by the open water test (Case01, 02 and 03) from the pre-sawn ice test (Case04 – Case21) at the same ship speed.

Figure 2 shows the measured ice force (Submerging + Velocity dependent force) in the different speed (Case04-Case12). The vertical axis shows the ice resistance in surge (Left figure) and heave (Right figure). The horizontal axis shows distance of ship advancing. In Figure 2, all of the length of the broken ices plate are 100mm. The measured data for ice thickness of 5mm, 10mm and 20mm are shown in Figures 2 (a), (b) and (c), respectively. The Red, Blue and Black lines show measured data in the ship speeds of high (0.392 m/s), middle (0.158 m/s) and low (0.040 m/s), respectively. In figures 2 (a), (b) and (c), the ice forces was gradually increasing with ship advancing distance after the first contact occurring at around x = 0.5m. The ice forces in surge strongly depend on the ship speed. The contact forces with the bow and the ice floe, which has velocity dependency, effects on the ice forces in surge. The fluid force for the rotating of the ice floe until the ice is paralleled to the bow plate of the advancing ship effects in the surge direction. On the other hand, the ice forces in heave shows weak dependency on the ship speed since the buoyancy force is dominant to the ice resistance in heave. The ice force in heave, therefore, can be approximately obtained by the sum of the buoyancy force of the ice floes submerging under the waterline. The ice force in surge becomes larger than that in heave in case of the high velocity. It is shown that the contributions of the velocity dependent force becomes larger than the buoyancy in the high velocity. The ice forces in both of directions increase with increasing the ice thickness. It is shown that the effect of the ice thickness in both directions are significant.

Figure 3 shows the ice force measured in the different ice length in order to investigate the effect of the length of the ice floe on the ice force (Case13-Case18). The dimension of the ices are 10mm in thickness × 50mm in length and 10mm in thickness × 200mm in length. The ice forces of the ice length of 50mm (Figure 3 (a)) shows the similar distribution to the ice length 100mm (Figure 2 (b)). It is shown that the ice length has less effect on the ice forces. The ice force distributions of the ice length of 200mm (Figure 3 (b)) however show a large difference from the ice force of the length of 50mm and 100mm. In the ice force for the ice length of 200m, it can be observed a number of the ices piled up at the bow plate. There a fewer ices drifting at ship's bottom and aft. The drifting of the ice floe, therefore, is affected by the geometrical conditions between the bow and the broken ice such as the bow angle, length and thickness of the ice as well as the ship speed. In Figure 3 (b), the ice force in surge of the ice length of 200m at low speed (black line) shows the repetitive peak force at 200mm interval. This interval of the peak force are clearly show the contact with the bow plate and the ice. It is shown that the contact force is dominant on the ice resistance in surge at the low speed.

Figure 4 shows the ice force measured in the conditions of the bow angle = 25° (Case19-Case21) in order to investigate the effect of the bow angle on the ice force (in Case04-Case18, the bow angle is 15°). The dimension of the broke ices is 10mm in thickness × 100mm in length which is same dimension as the Figure 2 (b). The ice force in surge measured in the case of the large angle (Figure 4, Left) is smaller than the ice force of the small angle (Figure 2 (b), Left). On the other hand, the ice force in heave measured in the case of the larger bow angle (Figure 4, Right) is larger than the ice resistance of the smaller bow angle (Figure 2 (b), Right). Generally the smaller bow angle increases the vertical component of ice contact (breaking) force, and decreases the horizontal component, so that the ice resistance in surge decreases and in heave increases. In Figure 4, the ice force related to the ice submerging, however, show opposite tendency to the ice contact force. It is assumed that the tendency obtained in Figure 4 is caused by the fluid force due to the rotating of the ice floes at the collision with the bow and the drifting of the ice floes along the bow, bottom and aft. The further investigations however are needed to clarify the contribution of the fluid force caused by ice rotating and the ice force caused by ice drifting.

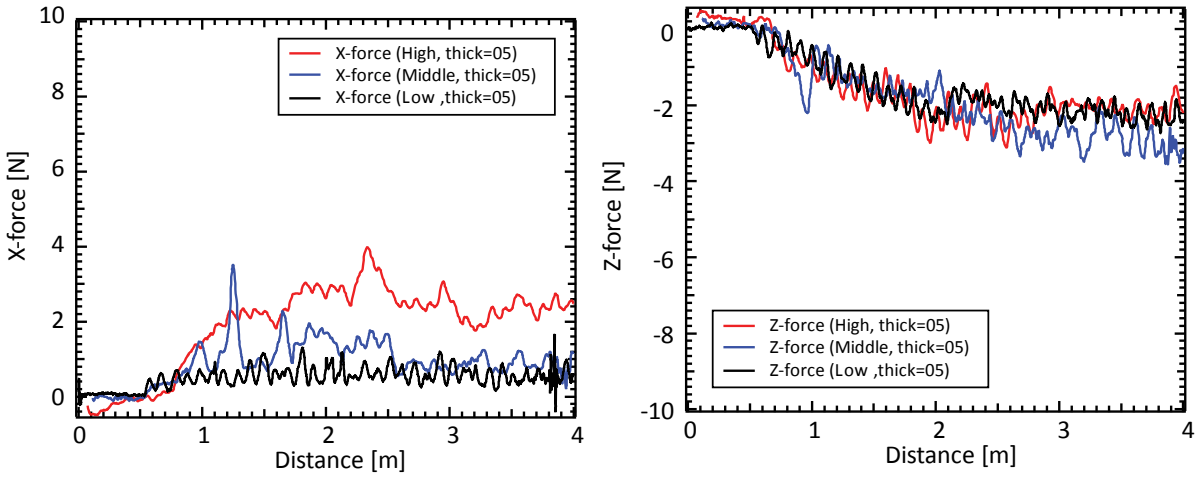

(a) Ice thickness = 5mm, length = 100mm (Black: Case 10 -Case 01, Blue: Case11-Case02, Red: Case12 - Case03)

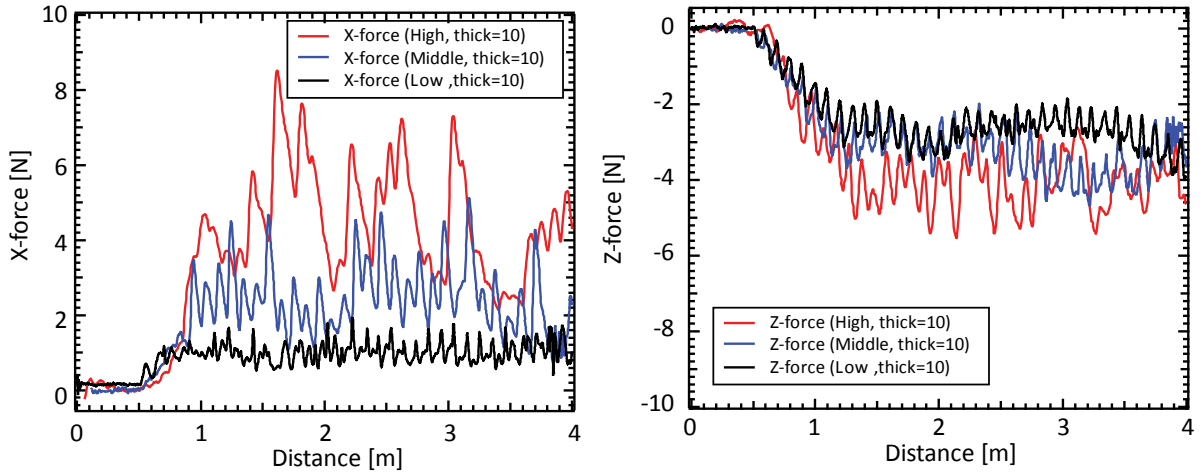

(b) Ice thickness = 10mm, length = 100mm (Black: Case 04 -Case 01, Blue: Case05-Case02, Red: Case06 - Case03)

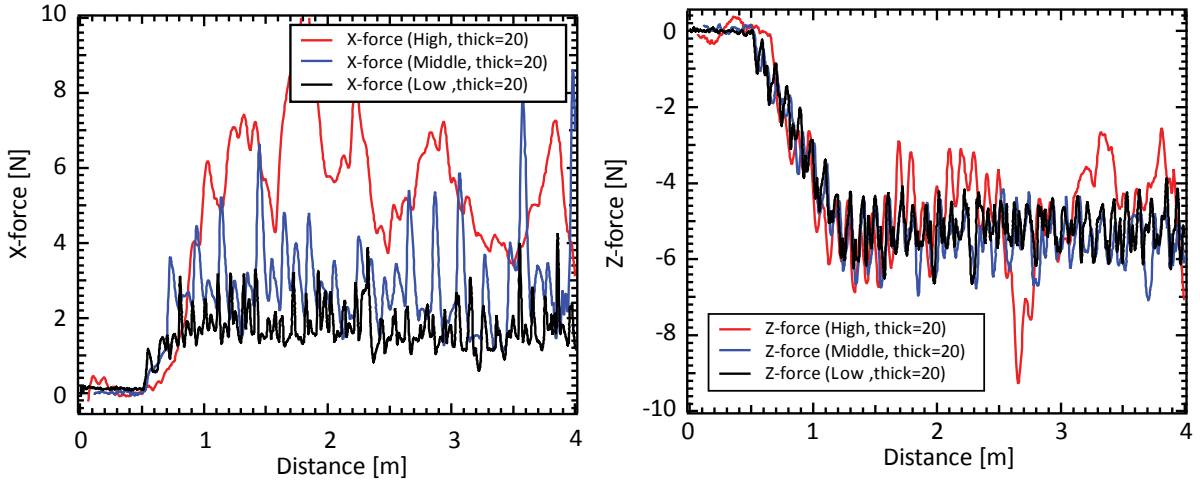

(c) Ice thickness = 20mm, length = 100mm (Black: Case 07 -Case 01, Blue: Case08-Case02, Red: Case09 - Case03)

Figure 2 Measured ice force (Submerging + Velocity dependent force)

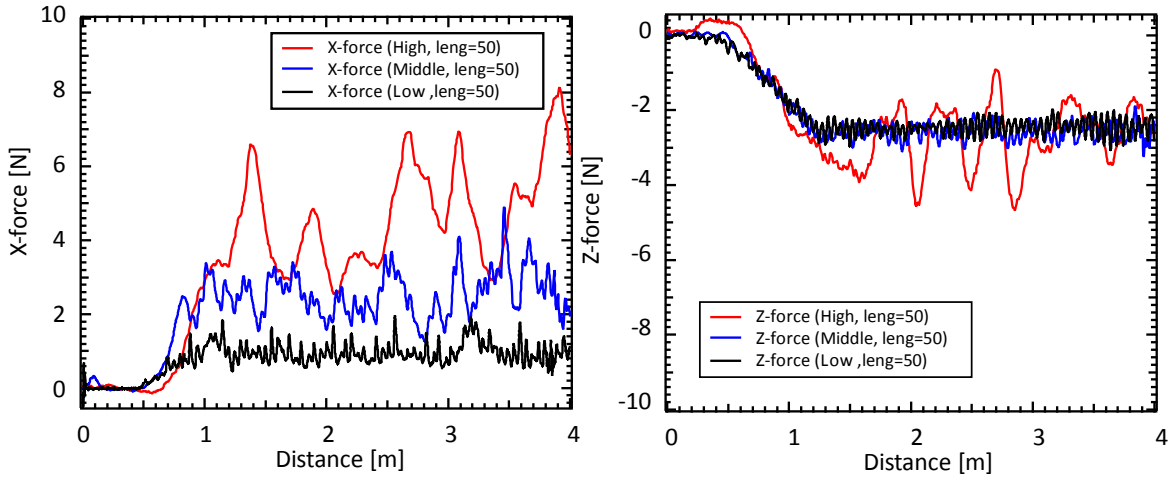

(a) Ice thickness = 10mm, length = 50mm (Black: Case 13 -Case 01, Blue: Case14-Case02, Red: Case15 - Case03)

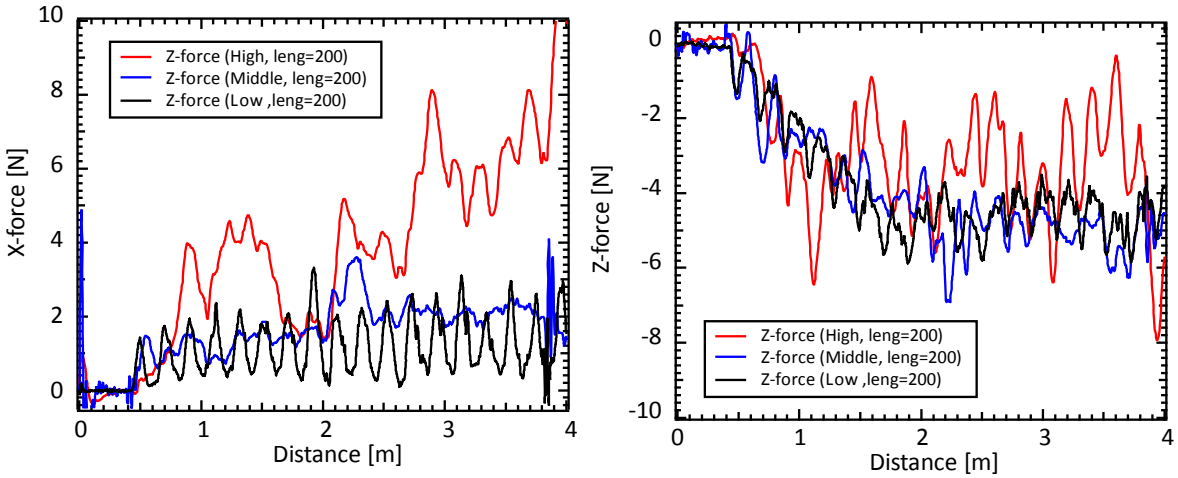

(b) Ice thickness = 10mm, length = 200mm (Black: Case 16 -Case 01, Blue: Case17-Case02, Red: Case18 - Case03)

Figure 3 Effect of the length of the broken ice on the ice force.

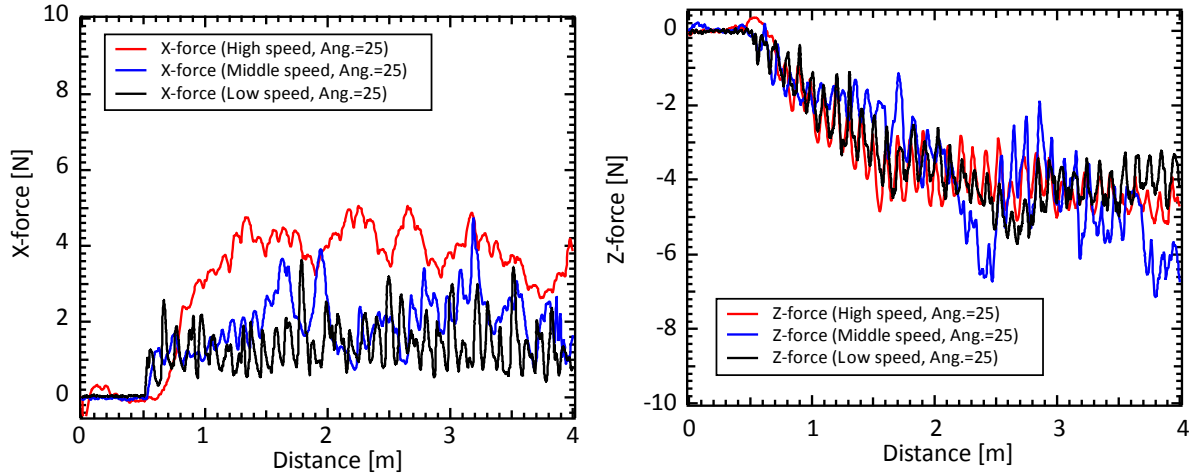

Figure 4 Effect of the bow angle on the ice force (Ice thickness=10mm, Length = 100mm, Black: Case19-Case01, Blue: Case20-Case02, Red: Case21-Case03).

The pre-sawn ice test using the synthetic ice provided the useful data to investigate the phenomena of the ice submerging. The ice force in surge is mainly induced by the fluid force for the ice rotating and the collision force between the bow plate and the ice. The dynamic response of the ice floes, which derives the velocity dependency in surge, are significant to the ice force at the high speed. The ice force in heave is mainly induced by the buoyancy of the ice floes, which derive less velocity dependency in heave. Therefore, the ice force in heave can be roughly estimated by the sum of the number of the ice floes drifting at the bottom, especially at the low speed. The effect of the ice thickness on the ice force is large, however, the effect of the ice length is small. The motion of the ice drifting is influenced by the geometrical conditions between the bow angle and the broken ice such as the length and thickness of the ice, so that the geometrical relationship between the hull shape and the size of the ice floes might be important for the ice resistance. More data are needed, however, to confirm these results.

NUMERICAL METHOD

A physically based modelling (e.g. Baraff, D., 1997) is applied to calculate the motions of ice floes due to the interactions between the ship and the ice floes. The ice floes are assumed to be a rigid body. A circle contact detection algorithm (e.g. Dimgliana *et al.*, 2000) is applied to detect the collision point between the ship and ice floe. The small contact circles are arranged on the ship's hull and the surface of the ice floe. The distance between the contact circles of the ship and the ice floes are calculated at each time interval Δt. The distance between two circles becomes zero at the collision point. The collision response between two objects (ship-ice, ice-ice) is calculated by an instantaneous impulse. The impulse vector $\mathbf{J}$ in the normal direction at the contact surface can be written as;

$$\mathbf{J} = j \cdot \mathbf{n}_{12}, \quad \text{where} \quad j = \frac{-(1+\varepsilon)v_{\text{ref}}}{\frac{1}{m_1} + \frac{1}{m_2} + \mathbf{n}_{12}\left\{\left(\mathbf{I}_1^{-1}(\mathbf{r}_1 \times \mathbf{n}_{12}) \times \mathbf{r}_2\right) + \left(\mathbf{I}_2^{-1}(\mathbf{r}_2 \times \mathbf{n}_{12}) \times \mathbf{r}_1\right)\right\}}, \tag{2}$$

where j is the magnitude of an impulse, $\mathbf{n}_{ik}$ is direction of an impulse force of the object i received from the object k, ε is a coefficient of restitution, v_{ref} is the relative velocity between two objects, m_i is the mass of an object i, and $\mathbf{I}_i$ is inertial tensor of an object i, and $\mathbf{r}_i$ is the displacement vector representing a displacement from the center of mass $\mathbf{x}_{gi}$ of an object i to the center of an contact circle $\mathbf{x}_{pi}$. A mechanical friction force of the Coulomb model is presented in the horizontal direction to the collision surface:

$$F_f = \mu \cdot F_c, \tag{3}$$

where μ is the kinematic friction coefficient between ship and ice. The direction of frictional force is opposite to the relative velocity between ship and ice. A fluid force of surrounding water acting on an ice floe is represented by:

$$\mathbf{F}_w = -C_D \cdot A \frac{1}{2} \rho |\mathbf{v}| \mathbf{v} \tag{4}$$

where C_D is the drag coefficient, A is a projected area, ρ is the water density and $\mathbf{v}$ is velocity of an ice floe. A direction of fluid force is opposite to the motion of the ice floe. In this paper,

the drag coefficient C_D is assumed to be 1.0. A buoyancy force at the gravity center of the ice floe is considered. For simplicity, other fluid forces related to ship motions are neglected. The motions of the ice floes are achieved by 3DOF rigid body equations. The position and orientation of the ice floe are solved by the Newton's second law. A position and orientation of the ice floe at each time step are computed by integrating the derivative equations.

The numerical simulations of ice submerging were carried out in the same conditions as the experiments. 2D model advances at the constant speed of 0.392m/s. The ice thicknesses are 5mm, 10mm and 20mm. The radius of the contact circles for the model and the ice are 5mm and 1.25mm, respectively. The time interval of the numerical integration Δt is 0.0001s.

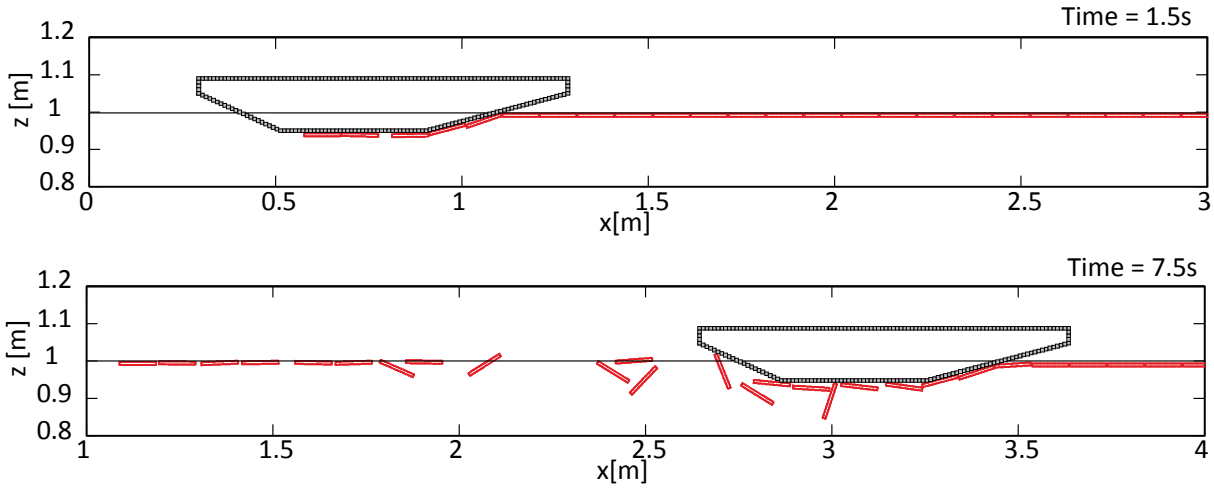

Figure 5 Calculated rotating and sliding of the ice floes (Ship speed = 0.392 m/s, Ice thickness = 10mm, Length of the ice = 100mm).

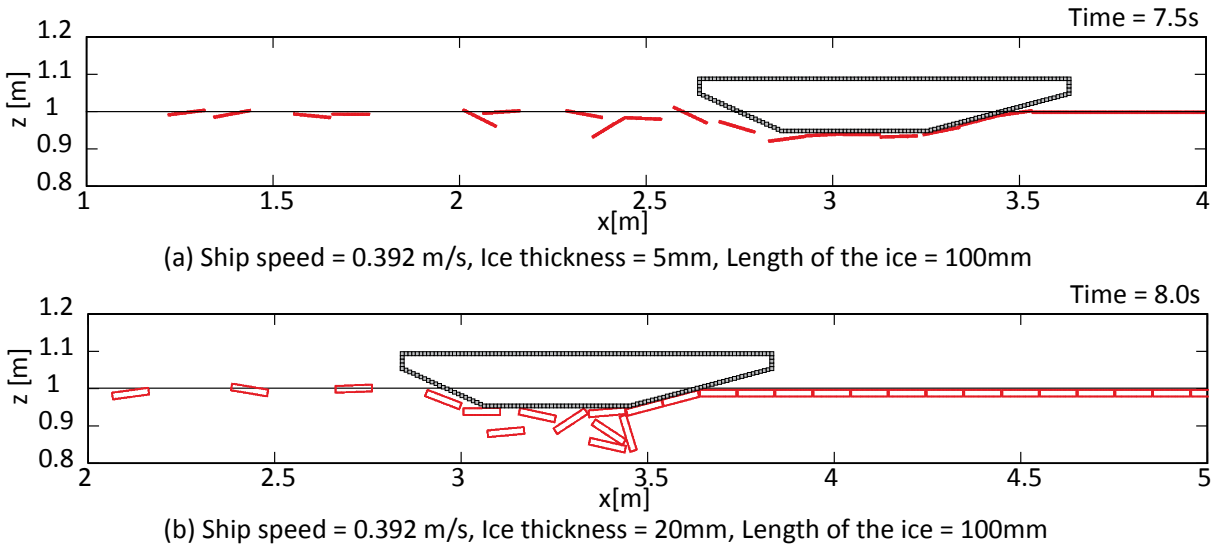

(a) Ship speed = 0.392 m/s, Ice thickness = 5mm, Length of the ice = 100mm

(b) Ship speed = 0.392 m/s, Ice thickness = 20mm, Length of the ice = 100mm

Figure 6 Calculated rotating and sliding of the ices floes in different ice thickness; (a) ice thickness = 5mm, (b) ice thickness = 20mm (Ship speed = 0.392 m/s, Length of the ice = 100mm).

Figure 5 shows the calculated ice submerging of the ice floes. The numerical conditions in Figure 5 are 10mm in thickness, 100mm in length. The ship velocity is 0.392m/s. Firstly, the ice collides with the bow, and is rotated by the ship further advancing until the ice is paralleled to the bow plate. Then, the ice floe is sliding along the bow plate, and drifting along the bottom plate. The ice drifting frequently shows the rotating at the bottom. Finally, the ice floe collides with the aft and is eliminated behind the ship. The numerical simulation can obtain detail of the drifting of the ice submerging as shown in Figure 5. Figure 6 shows the submerging of the ice floes in different ice thickness. The ice thickness in Figure 6 (a) and (b) are 5mm and 20mm, respectively. The both of the ice length is 100mm. In Figure 6, the differences are shown in the ice drifting at the bottom between ice thicknesses of 5mm in Figure 6 (a), 10mm in Figure 5 (b) and 20mm in Figure 6 (b). The ice drifting is affected by the fluid force acting on the ice floe and the geometrical conditions such as the bow angle and the ice thickness. However, in the numerical simulations, the fluid force induced by the ship advancing are neglected in the motion of the ice floes.

Figure 7 shows the calculated ice force distributions of the ice submerging in different ice thickness. The numerical conditions are same as Figures 5 and 6. The time interval of an impulsive response is assumed to be 0.05s, which is used to transfer from impulsive response [N·s] to the peak force [N]. In Figure 7, the left figure shows the ice force in surge, and the right figure shows the ice force in heave. The ice force distribution both directions of heave and surge increases with increasing the ice thickness which is similar tendency to the experimental results. The calculated ice force in heave roughly agrees with the experimental data qualitatively. In Figure 7 (c), the ice force in heave of 20mm ice thickness show the large peak force, in which several of ices drifting on the bottom piles up and collide with the ship at the same time, which cannot be observed in the experiments. On the other hand, the calculated ice force in surge is relative smaller than the experimental ice force since the fluid force induced by the ship advancing are neglected in the numerical model. The numerical model, therefore, has to be consider the hydrodynamic effect acting on the ice floe such as ventilation. More detail investigations with experimental and the numerical data are needed to estimate submerging force and velocity dependent force quantitatively.

CONCLUSIONS

The ice submerging after an icebreaker breaks a floating ice cover was investigated both experimentally and numerically. 2D model tests using the polypropylene's synthetic ice were carried out to provide information of ice submerging such as the ice force and motions of the broken ice floes. 2D numerical model that enables simulations of ice force on the icebreaker advancing into pre-sawn ices was developed. The numerical results are compared with experimental data.

1) The pre-sawn ice test using the synthetic ice can obtain useful data to investigate the ice submerging force and velocity dependent force. The ice force in surge shows strong dependency on the ship speed. On the other hand, the ice force in heave shows weak dependency on the ship speed and can be roughly estimated by the buoyancy of the ices. The geometrical conditions between the hull shape and the size of the ice floes affect the drifting of the ice floes, which has important role of velocity dependence force.

2) The calculated ice force of the ice submerging roughly agreed with the experimental data. However, the calculated ice force in surge is underestimated because of the neglecting the hydrodynamic force induced by a ship advancing such as ventilation.

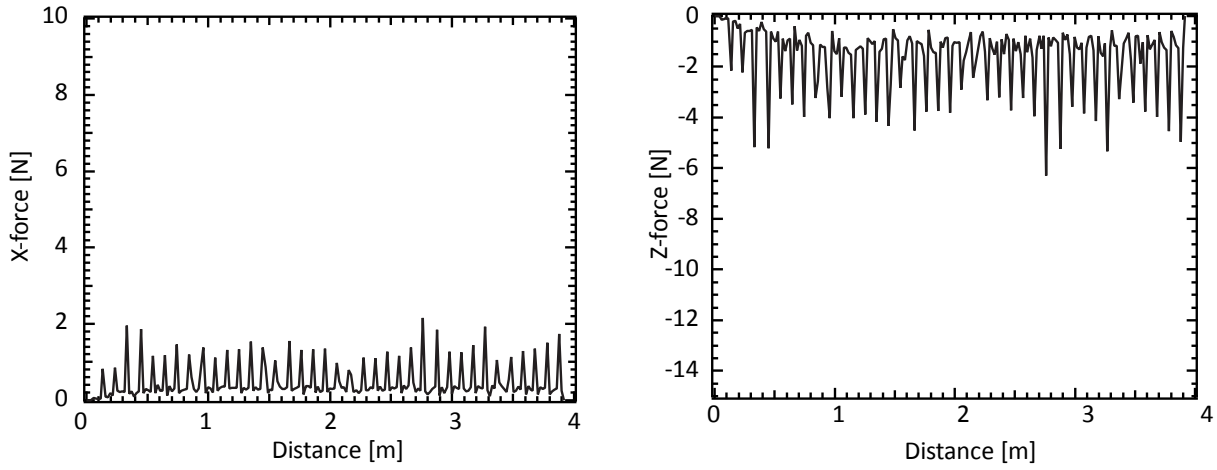

(a) Ship speed = 0.392 m/s, Ice thickness = 5mm, Length of the ice = 100mm

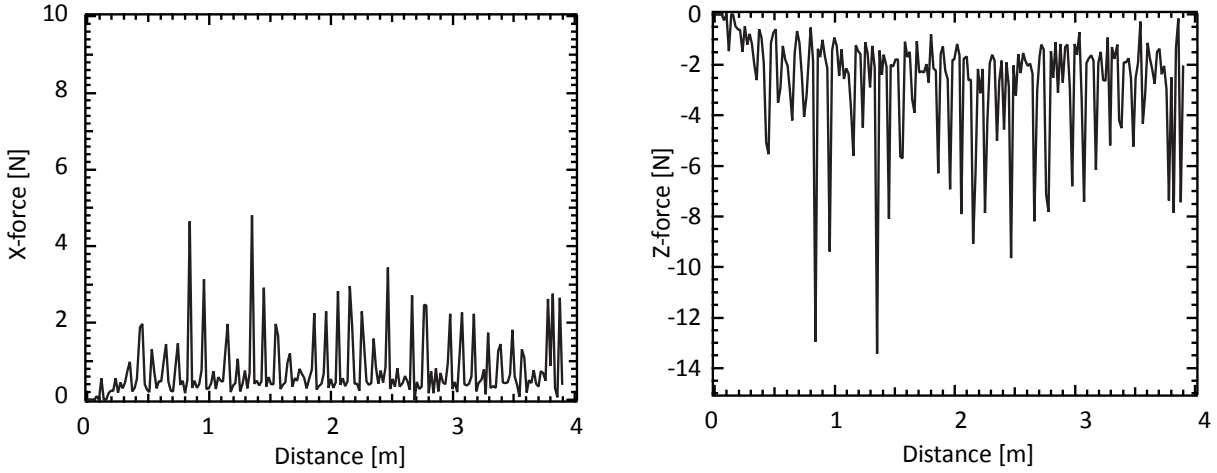

(b) Ship speed = 0.392 m/s, Ice thickness = 10 mm, Length of the ice = 100mm

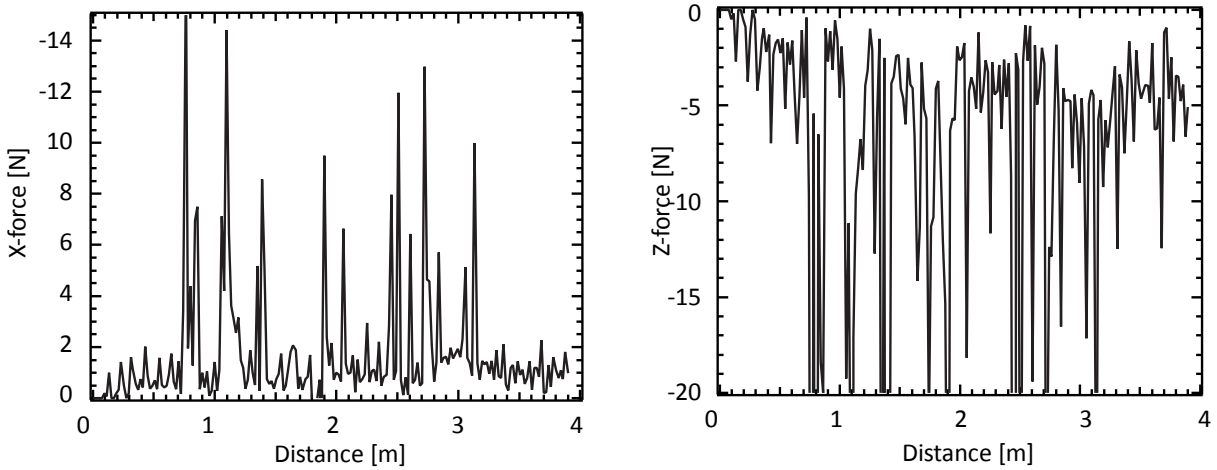

(c) Ship speed = 0.392 m/s, Ice thickness = 20 mm, Length of the ice = 100mm

Figure 7 Calculated ice force distribution for ice submerging in different ice thickness; (a) ice thickness = 5mm, (b) ice thickness = 10mm, (c) ice thickness = 20mm (Ship speed = 0.392 m/s, Length of the ice = 100mm).

3) The hydrodynamic force induced by the ice submerging are important role to estimate the ice force as well as friction force. Further investigations are need to estimate submerging force and velocity dependent force both numerically and experimentally.

ACKNOWLEDGEMENTS

This research was supported by JSPS KAKENHI Grant Number 25289316, 26630455 and Shipbuilders' Association of Japan (SAJ). The support of both organization is greatly acknowledgement. Authors would like to thank Mr Tsuyoshi Endo, Nippon Data Service Co., Ltd., for great assistance in the model tests.

REFERENCES

Baraff, D., 1997. Rigid Body Simulation I and II. Siggraph 97, Course notes.

Dimgliana, J. and O'Sullivan, C., 2000. Graceful degradation of collision handling in physically based animation, Computer Graphics Forum, Vol. 19, Issue 3, pp 239-248.

Enkvist, E., 1972. On the Ice Resistance Encountered by Ships Operating in the Continuous Mode of Icebreaking, The Swedish Academy of Engineering Sciences in Finland, Report No.24.

Frederking, R., 2003. Determination of Ice Pressure from Ship Transits in Ice. Proceeding of the 13th International Offshore and Polar Engineering Conference, Vol. 1, pp 484.

Izumiyama, K., Wako, D., and Uto, S., 1999. Ice Force Distribution Around a Ship Hull. Proceeding of the 21th International Conference on POAC, Vol. 4, pp 707.

Konno, A., and Mizuki, T., 2006. Numerical Simulation of Pre-sawn Ice Test of Model icebreaker using physically based modelling. Proc. 18th IAHR International Symposium on Ice, pp 17.

Puntigliano, F. M., 1997. On the ship resistance under the design waterline in the continuous mode of icebreaking in level ice. OMAE, Vol. 4, Arctic/Polar Technology ASME, pp 73.

Sawamura J., and Tachibana T., 2011. Development of a Numerical Simulation for Rotating and Sliding of the Ice Floes along the Ship hull, Proc. 21st International Conference on Port and Ocean Engineering under Arctic Conditions, POAC11-036

Sawamura J., 2015. Numerical Study on Ice Force Distribution for Plate Ice Failure and Broken Ice Submerging for Ship Maneuver in Level Ice. Proc. 22nd International Conference on Port and Ocean Engineering under Arctic Conditions, pp 171.

Song Y.Y., Kim M.C., and Chun H.H., 2007. A Study on Resistance Test of Icebreaker with Synthetic Ice. Journal of the Society of Naval Architects of Korea, Vol.44, No.4, pp 389.

Valanto, P., 1992. The icebreaking problem in two dimensions: Experiments and Theory, Journal of Ship Research, Vol. 36, No. 4, pp. 299.